



Radiation defects in SrLaGa₃O₇ crystals doped with rare-earth elements

S.M. Kaczmarek ^{a,*}, R. Jabłoński ^b, I. Pracka ^b, G. Boulon ^c, T. Łukasiewicz ^{b,d},
Z. Moroz ^e, S. Warchoń ^f

^a Institute of Optoelectronics, M.U.T., 2 Kaliski Str., Warsaw, 01-489, Poland

^b Institute of Elec. Materials Technol., 133 Wólczyńska Str., Warsaw, 01-919, Poland

^c Laboratoire de Phys.-Chimie des Matériaux Luminescentes, 69622 Villeurbanne Cedex, France

^d Institute of Applied Physics, M.U.T., 2 Kaliski Str., Warsaw, 01-489, Poland

^e Sołtan Institute of Nuclear Studies, 05-400 Świerk, Poland

^f Institute of Chem. and Nuclear Technics, 16 Dorodna Str., Warsaw, 02-415, Poland

Received 15 December 1997; received in revised form 25 May 1998

Abstract

Influence of γ and proton exposures on the optical absorption and photoluminescence of SrLaGa₃O₇ (SLGO) single crystals doped with Nd, Dy and Pr was studied. We observed that color centers, which appeared after the irradiation, shift the short-wave absorption edge towards the longer wavelengths by a few hundreds nm. They are probably attributed to the Ga³⁺ centers which are formed according to the reaction $\text{Ga}^{3+} + e^- \rightarrow \text{Ga}^{2+}$ with a spin of $S = \frac{1}{2}$, $g_{\parallel} = 1.9838(5)$ and $g_{\perp} = 2.0453(5)$. © 1998 Elsevier Science B.V. All rights reserved.

PACS: 61.72.Ji; 61.80.Ed; 42.70.Iij

Keywords: Radiation defects; Rare-earths; Color centers

1. Introduction

Single crystals of SrLaGa₃O₇ (SLGO) exhibit the highest structural homogeneity among all melilites compounds [1,2]. They appear to be promising active laser materials [3,4]. They exhibit, however, strong changes in absorption and luminescence spectra under irradiation by ionizing par-

ticles. These changes influence properties of lasers in which the SLGO crystals are used as the active material.

In the present work we attempted to study in more detail the influence of gamma and proton radiation on the optical properties of Nd-, Dy- and Pr-ion doped SLGO crystals.

2. Experimental

The detailed description of the applied growth process is presented in papers [5,6].

* Corresponding author. Tel.: 00 48 22 6859019; fax: 00 48 22 6668950; e-mail: laslab@wat.waw.pl.

2.1. Radiation sources

Gamma-ray irradiation of the samples was performed with a ^{60}Co source at a rate of 1.5 Gy up to an absorbed dose of 10^6 Gy. For proton irradiation a cyclotron was used. The average energy of protons was about 26 MeV and the fluence of 10^{13} – 10^{16} particles cm^{-2} .

2.2. Spectroscopic investigations

To obtain optical absorption coefficients in the range of 200–1100 nm, transmission spectra of the samples were measured before and after γ and proton irradiation using a LAMBDA-2 Perkin-Elmer spectrophotometer. Samples of SLGO crystals doped with Nd (5 and 10 at.%), Pr (1, 0.5 at.%) and Dy (1, 0.5 at.%) with diameters of 10 mm and a thickness of 1–2 mm were cut out perpendicularly to the growth axis. Samples in the form of a rod of 4 mm diameter and about 36 mm long were also investigated. We obtained the change $\Delta K(\lambda)$ in the optical absorption coefficient:

$$\Delta K(\lambda) = \frac{1}{d} \ln \frac{T_1}{T_2}, \quad (1)$$

where λ is the wavelength, d the sample thickness and T_1 and T_2 are the transmissions of the sample obtained before and after gamma irradiation, respectively.

2.3. ESR investigations

The samples, typically of $3.5 \times 3.5 \times 2$ mm³, were measured in a BRUKER ESP-300 ESR spectrometer (X-band). The spectrometer was equipped with a helium flow cryostat (type ESR-900 Oxford Instruments). The ESR lines were observed before and after gamma exposure of 10^5 Gy dose in a temperature range from 4 to 300 K using microwave powers from 0.002 to 200 mW. Moreover, above investigations were performed for crystals annealing in air at 800°C for 3 h.

3. Results

3.1. Spectroscopic investigations

Additional absorption (AA) bands observed in the Nd : SLGO and Pr : SLGO crystals after γ irradiation with a dose of 10^5 Gy and in the Dy : SLGO crystals with a dose of 10^6 Gy are shown in Fig. 1. As seen, in SLGO crystals doped with Dy, Nd and Pr the gamma induced AA bands appear at about 290 and 380 nm, and the first one is much stronger than the second one. Their intensity depends on the gamma dose and on the kind of the impurity. With increasing Pr or Dy concentration, the intensity of the 290 nm band decreases, but with the increasing the Nd concentration, it also increases. In Fig. 1 one can see also the AA bands for the Nd : SLGO (5 at.% of Nd³⁺) rod (curve 3), in comparison with that for a 2.1 mm plate (curve 2).

Moreover, red-shift of the short-wave absorption edge by about 50 nm is induced by gamma irradiation of a thin SLGO sample. The value of the shift strongly depend on gamma dose and sample thickness.

Fig. 2 presents changes in transmission spectrum (Fig. 2(a)) of “as grown” Dy : SLGO crystal (1 at.%) (curve 1) after treatments: gamma irradiation with a dose of 10^6 Gy (curve 2), thermal annealing in air at 1200°C for 3 h (curve 3) and γ exposure with a dose of 10^3 Gy (curve 4) and AA bands induced by γ exposure (Fig. 2(b)). One can see a shift of the short-wave absorption edge and two different radiation optical absorption bands, with a maximum at 380, and at 290 nm. The first of these defects appear mainly after previous annealing of the crystal and next γ -exposure. It is concerned to curve 5 from Fig. 1 (Pr : SLGO (0.5 at.%) as well as to curve 4 from Fig. 2(a) (Dy : SLGO (1 at.%)

The Dy : SLGO crystal (0.5 at.%, $d=2.91$ mm) was irradiated also by protons with a doses from 10^{13} to 10^{16} cm^{-2} . Dose dependence of additional absorption in Dy : SLGO crystal is presented in Fig. 3. Three regions are seen. First, for doses $<10^{14}$ cm^{-2} , where an increase in AA is seen, second for doses near 10^{14} cm^{-2} , where saturation and subsequent decrease of AA is observed and

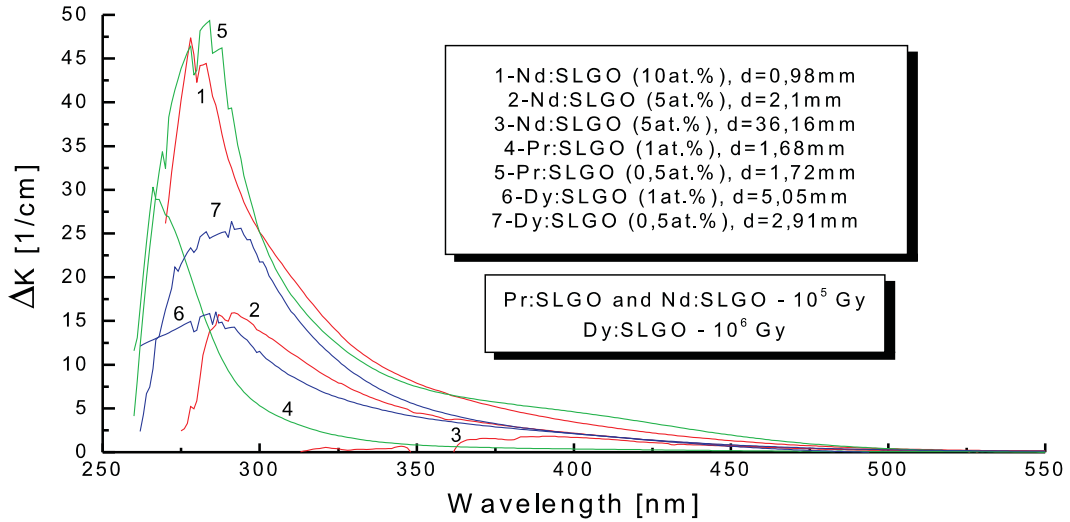


Fig. 1. Additional absorption bands of Dy, Pr and Nd doped SLGO crystals after gamma irradiation with doses of 10^5 (Pr and Nd : SLGO) and 10^6 Gy (Dy : SLGO).

third for doses $>10^{14}$ cm $^{-2}$, where again an increase of AA takes place. AA bands were obtained at 270 and 370 nm [7]. This is the same picture as that related to the changes induced in the same crystal by gamma's with a dose of 10^6 Gy. Thus,

we conclude we have dealing with the same radiation defect.

This situation is described much more clearly in Fig. 4, where changes in the transmission registered for the Nd : SLGO (5 at.%) rod of the length

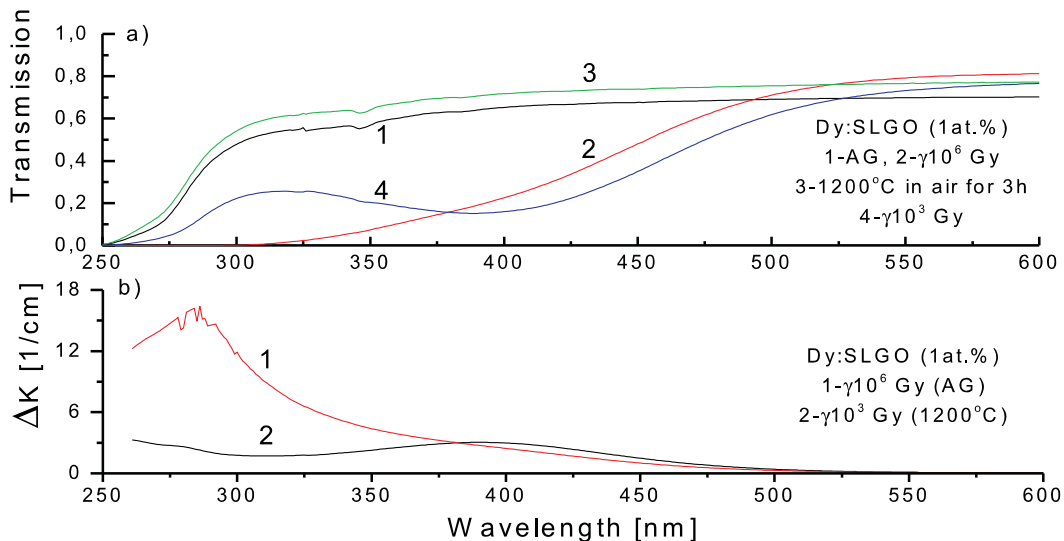


Fig. 2. Changes in transmission spectrum (a) of 'as grown' Dy : SLGO crystal (1 at.%) (curve 1) after subsequent: gamma irradiation with a dose of 10^6 Gy (curve 2), thermal annealing in air at 1200°C for 3 h (curve 3) and gamma exposure with a dose of 10^3 Gy (curve 4) and AA bands after γ exposure (b): after γ 10^5 Gy (curve 1) and γ 10^3 Gy (curve 2).

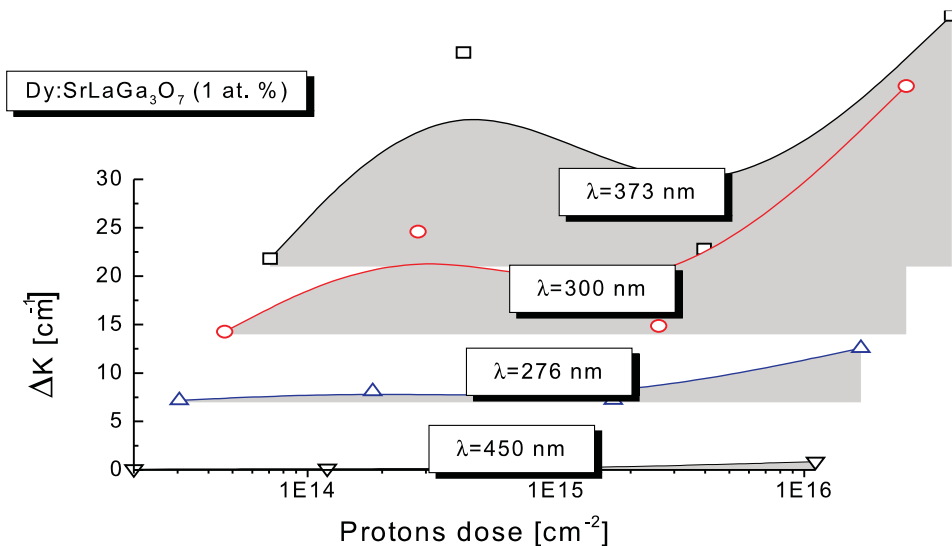


Fig. 3. Dose dependence of AA after proton exposure of Dy : SLGO crystal.

of 36.16 mm for different gamma doses are shown. This rod was subsequently irradiated by gamma rays with 10^4 Gy, annealed at 400°C for 3 h, irradiated with 10^5 Gy, annealed at 1200°C for 3 h and, finally, irradiated with 10^5 Gy. The wavelength for which the transmission value reach the level of 0.001 was taken as a short-wave absorption edge. As seen from the figure, this edge be-

came shifted with the increase of the radiation dose towards the longer wavelengths. This linear shift (Fig. 4(b)), for the rod of about 36 mm length and 10^6 Gy, may even be as large as 120 nm. For as grown crystal (curve 1) additional band is seen between 300 and 350 nm, which disappear partially after γ exposure and totally after thermal annealing at 1200°C .

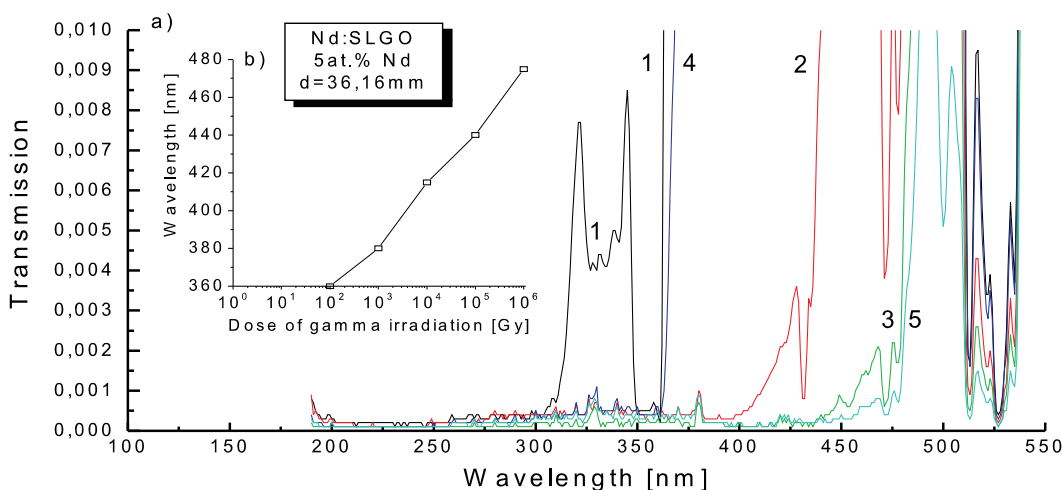


Fig. 4. Transmission spectra for the Nd : SLGO (5 at.%) rod of 36, 16 mm length for different types of treatments: 1-AG, 2- 10^4 Gy, 3- 10^5 Gy, 4- 1200°C for 3 h in air, and 5- 10^5 Gy (a) and linear dose dependence of short-wave absorption edge shifting (b).

In the photoluminescence spectrum of Nd : SLGO (5 at.%) crystal we have seen changes in relative values of a photoluminescence close to $\lambda = 910$ nm. The appearance of the two irradiation defects result also from thermoluminescence measurements [7].

3.2. ESR investigations

ESR measurements revealed an anisotropic spectrum is observed after 10^5 Gy gamma exposure of SLGO crystal. This spectrum possesses two lines with linewidth of $\Delta H_{pp} = 3$ mT. For plane (0 0 1) the g -factor has values in the range of 2.0045–2.044. Its angular dependence is depicted in Fig. 5.

Moreover g -factor for the orientation parallel to c -axis is equal to 2.025. These lines are observed at temperatures from 4 to 300 K but are combined into an isotropic single line above 227 K, due to line broadening, as seen in Fig. 6. After about 600 h of storage at room temperature, the amplitude of the ESR signal decreases by a factor of 10 with a decay time constant of 264 h. Moreover, after 3 h annealing of the crystal at 400°C in air these lines disappear.

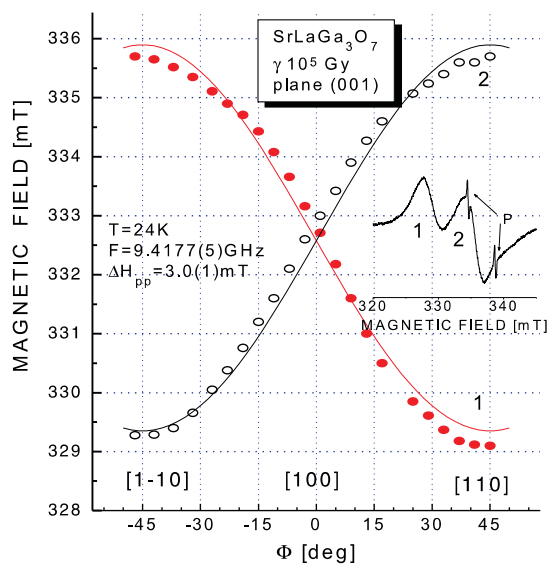


Fig. 5. Angular dependence of radiation defect in (0 0 1) plane of SLGO crystal. Inside ESR spectrum for [1 1 0] direction.

pear. The above mentioned lines appears after γ -irradiation, independent on the kind of impurity, also in the undoped SLGO crystal.

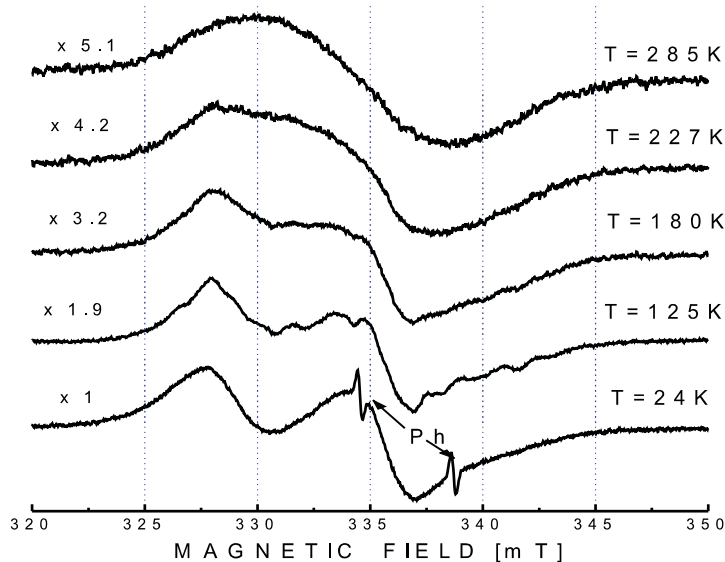


Fig. 6. Temperature dependence of ESR lines for Dy^{3+} : SLGO crystal after γ -irradiation with a dose of 10^5 Gy.

4. Discussion

After gamma and protons irradiation of SLGO crystals doped with Dy, Nd and Pr optical absorption bands appear, located at about 290 and 380 nm. Their intensities depends on gamma's and proton dose. From Fig. 3 it results that the optical absorption bands that appear in the dose range of 10^{13} – 10^{14} cm^{-2} and disappears by further irradiation are due to recharging of existing defects and those that appear at higher doses are due to Frenkel pair formation.

Comparison of ESR and optical results point us to the hypothesis that 290 nm band can shifts short-wave absorption edge towards the longer wavelengths. Fig. 7 shows the crystallographic positions of La^+ , Ga^{3+} , Sr^{3+} and O^{2-} ions in the SLGO lattice (*C* axis projection). In this figure we see six $T1, T2 \dots T6$ of GaO_4^{2-} type tetrahedral, where large circles design Ga^{3+} ions, small ones O^{2-} ions and the largest are Sr^{3+} or La^+ cations.

The obtained ESR spectra can be explained by means of the following process: Ga^{3+} ion captures the electron which was released from O^{2-} ion by γ or proton radiation and in a consequence, Ga^{2+} paramagnetic center is formed with a spin value equal to $S = \frac{1}{2}$. In that way tetrahedron distortion arises along $\text{Ga}^{2+}-\text{O}^{1-}$ (ionic radius of O^{2-} is equal to 1.32 Å while O^{1-} is 1.76 Å) axis. This situation is described in Fig. 8.

The process of the formation of this paramagnetic center can be illustrated by the following reactions: $\text{O}^{2-} + \gamma \rightarrow \text{O}^{1-} + e^-$; $\text{Ga}^{3+} + e^- \rightarrow \text{Ga}^{2+}$.

The measured angular dependencies of ESR lines show that this process inside $T1$ tetrahedron takes place and suggest that $T1$ configuration is energetically the most favorable for this kind of process. Favorable position of $T1$ tetrahedral with respect to the above process is connected with local symmetry of the crystal field. It demands more investigations.

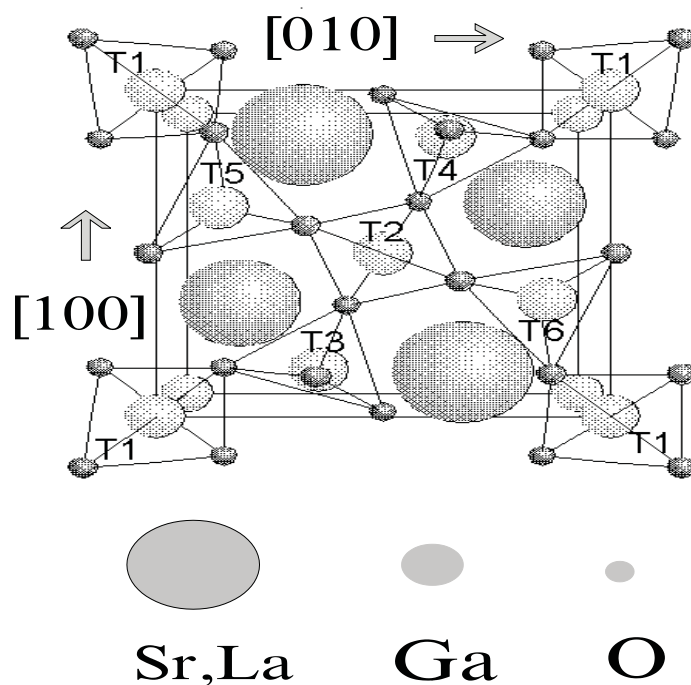


Fig. 7. Crystallographic positions of Sr^{3+} , La^+ , Ga^{3+} and O^{2-} ions in SLGO lattice.

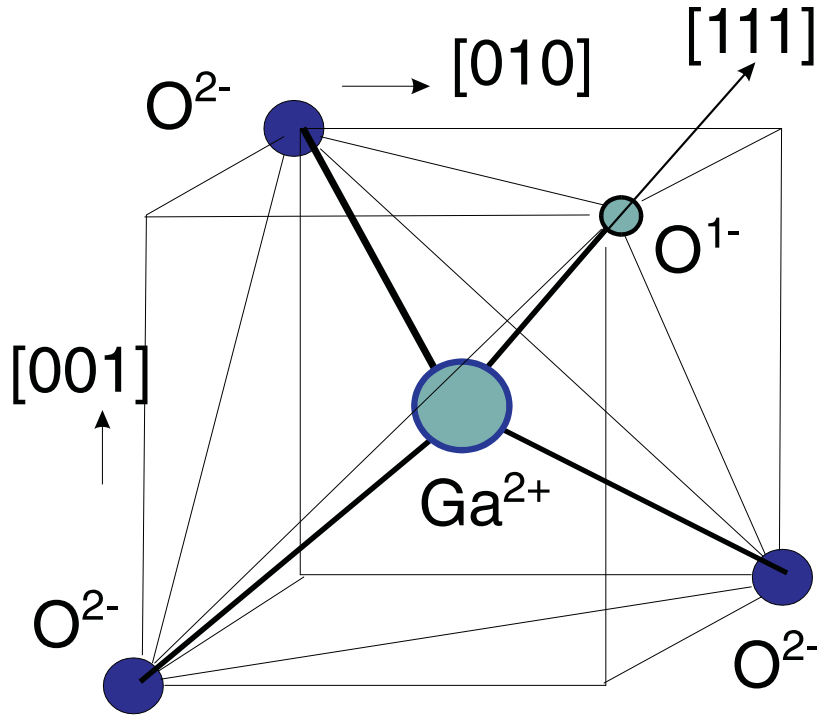


Fig. 8. Complexes of $(\text{Ga-O})^{1-}$ arising in SLGO structure ($T1$ tetrahedron) after γ - or proton irradiation.

In this situation the spin Hamiltonian we can write in the form

$$H = g\beta HS, \quad (2)$$

where $S = \frac{1}{2}$, $H_{\text{rez}} = \nu/(g\beta h)$, $g^2 = g_{\perp}^2 \sin^2 \theta + g_{\parallel}^2 \cos^2 \theta$, β – Bohr magneton, θ – angle between magnetic field and axis of a center, h – Planck constant, g – Lange factor and H_{rez} – magnetic field. Because the direction of an axis each of 4th $(\text{Ga-O})^{1-}$ complexes inside $T1$ tetrahedron is of $[1\ 1\ 1]$ type and maximum H_{res} is directed along $[1\ 1\ 0]$, that is $\varphi = 45^\circ$ in $(0\ 0\ 1)$ plane, we can obtain

$$\begin{aligned} g_{\parallel}^2 &= 2g_{[1\ 1\ 0]}^2 - g_{[1\ 0\ 0]}^2 \quad \text{and} \\ g_{\perp}^2 &= 2g_{[1\ 0\ 0]}^2 - g_{[1\ 1\ 0]}^2. \end{aligned} \quad (3)$$

From angular dependence (Fig. 5) we obtained: $g_{[1\ 0\ 0]} = 2.025$ and $g_{[1\ 1\ 0]} = 2.0045$ or 2.044 , and using Eq. (3) we have obtained: $g_{\parallel} = 1.9838(5)$ and $g_{\perp} = 2.0453(5)$.

5. Conclusions

After γ and proton irradiations of the SLGO crystal doped with Pr, Dy and Nd, as well as undoped ones, AA bands appear in the absorption spectra, with maxims at about 290 and 380 nm. Location and intensity of the first band depends on the type of impurity and value of irradiation dose.

With increasing Pr or Dy concentration, maximum intensity of this band decreases, but with increasing the Nd concentration, it increases. An increase of Pr concentration shift this maximum towards the shorter wavelengths. Therefore, intensity and location behavior of this band as a function of impurity concentration strongly depend on the type of impurity.

The 380 nm band appear mainly after previous annealing of the SLGO crystal in air and is probably connected with recharging effect of oxygen vacancies.

For the 290 nm AA band the next phenomenon probably take place: as a result of ionizing radiation, paramagnetic centers are formed according to the reaction $\text{Ga}^{3+} + e^{-} \rightarrow \text{Ga}^{2+}$.

References

- [1] A.A. Kaminskii, E.L. Belokoneva, B.V. Mill, S.E. Sarkisov, K. Kurbanov, *Phys. Status Solidi A* 97 (1986) 279.
- [2] L.R. Black, D.M. Andrauskas, G.F. de la Fuente, H.R. Verdun, *Proc. SPIE* 1104 (1989) 175.
- [3] W. Ryba-Romanowski, S. Gołąb, G. Dominiak-Dzik, M. Berkowski, *Mater. Sci. Eng. B* 15 (3) (1992) 217.
- [4] S. Kaczmarek, Z. Mierczyk, K. Kopczyński, *Opto-electronics Review* 2 (1993) 54.
- [5] I. Pracka, W. Giersz, M. Świrkowicz, A. Pajączkowska, S. Kaczmarek, Z. Mierczyk, K. Kopczyński, *Mater. Sci. Eng. B* 26 (2/3) (1994) 201.
- [6] I. Pracka, M. Malinowski, K. Kopczyński, S. Kaczmarek, Z. Mierczyk, M. Świrkowicz, J. Kisielewski, T. Łukasiewicz, *Proc. SPIE* 3178 (1997) 42.
- [7] S.M. Kaczmarek, R. Jabłoński, I. Pracka, G. Boulon, T. Łukasiewicz, Z. Moroz, S. Warchoń, *Biul. WAT* 12 (1997) 133.